

## Like-charge colloidal attraction: A simple argument

E. TRIZAC

*Laboratoire de Physique Théorique et Modèles Statistiques, UMR CNRS 8626  
Université Paris-Sud - 91405 Orsay, France*

L. ŠAMAJ

*Institute of Physics, Slovak Academy of Sciences - Dúbravská Cesta 9, Bratislava 84511, Slovakia*

**Summary.** — By a length scale analysis, we study the equilibrium interactions between two like-charge planes confining neutralising counterions. At large Coulombic couplings, approaching the two charged bodies leads to an unbinding of counterions, a situation that is amenable to an exact treatment. This phenomenon is the key to attractive effective interactions. A particular effort is made for pedagogy, keeping equations and formalism to a minimum.

### 1. – Introduction

Consider two identically charged macromolecules alone in an electrolyte, and assume that Coulombic forces exclusively are at work. By integrating out the microscopic degrees of freedom (the electrolyte), one obtains the effective pair potential between the two macromolecules [1]: is it attractive or repulsive? Of course in vacuum (*i.e.* without the electrolyte), the two bodies always repel, but the presence of the electrolyte complicates the matter, to such an extent that the answer to the above question has been a rather

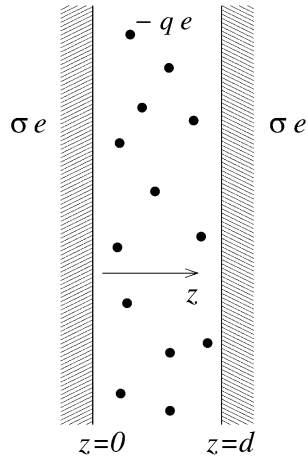


Fig. 1. – Sketch of the geometry considered, and definition of relevant parameters. The two charged parallel plates at distance  $d$  are neutralised by counterions of charge  $-qe$ , represented by the black dots. The system can be viewed as a minimal model where like-charge attraction may be present, in some adequate range of distance and coupling.

controversial subject since at least the 1930s [2-5]. In essence, all early contributions pertained to mean-field, a treatment for which it can be rigorously shown that the effective potential is repulsive [6-8]. Yet, it has been understood since the 1980s that like-charge attraction is nevertheless possible [9-11]. Since this phenomenon is a signature of non-mean-field effects, it is not straightforward to build an intuitive picture of the underlying mechanisms. It is our goal here to present a simple argument where the prerequisite for like-charge attraction become clear, and which provides exact results in some limiting sense to be made precise below (namely for short distances and large couplings).

The paper is organised as follows. We first lay out the model in sect. **2** where the contact theorem is also reminded. It is the cornerstone of our analysis. We then analyse the limiting case where the two macromolecules are distant (sect. **3**), which sheds interesting light on the physics at work when the two plates are close, as developed in sect. **4**. Our results are further discussed in sect. **5** and conclusions are finally drawn in sect. **6**.

## 2. – The model

We shall concentrate on the simplest setting possible, that where the two macromolecules (colloids) are envisioned as two parallel planar surfaces at a distance  $d$ , see fig. 1. Each colloid/plate is assumed to bear a uniform surface charge distribution  $\sigma e$ , where  $e$  is the elementary charge. The solvent is a structureless medium of dielectric permittivity  $\epsilon$ , the same as the permittivity of the macromolecules themselves (dielectric image effects are discarded) and the system is in equilibrium at temperature  $T$ . In between the colloids, mobile counterions of charge  $-qe$  ensure global electro-neutrality. While the microscopic density of counterions is strongly modulated (ions repel), the

coarse-grained density profile  $\rho(z)$ , averaged over a plane at a given position  $z$ , is a smooth function. For the sake of the argument, the counterions are assumed point-like: usually, a hard core is required to prevent collapse of oppositely charged small ions, but we deal here with a system having one type of small ions only, all of the same charge (no salt), and that is therefore free of divergences. From the permittivity  $\epsilon$  and temperature  $T$ , we define the so-called Bjerrum length  $\ell_B = e^2/(\epsilon kT)$  as the distance where the repulsion between two elementary charges coincides with thermal energy  $kT$  ( $k$  is Boltzmann's constant, and we use CGS units, so that for water at room temperature, one has  $\ell_B \simeq 7 \text{ \AA}$ ). Note that global electro-neutrality imposes the following constraint on the counterion profile:  $\int_0^d \rho(z) dz = 2\sigma/q$ .

The question is: what is the sign of the pressure  $P$ , *i.e.* the force between the two plates per unit surface? To find the answer, it is essential here to invoke a key result, known as the contact theorem [12]. It states that  $P$  is, quite intuitively, the sum of two contributions:

$$(1) \quad P = \rho(0)kT - \frac{2\pi}{\epsilon} \sigma^2 e^2.$$

The first one,  $\rho(0)kT$ , is repulsive and stems from the collisions of counterions with the plate. The second,  $2\pi\sigma^2 e^2/\epsilon$ , is the traditional electrostatic pressure, important in capacitor physics. It is attractive, and simply means here that the plate located at  $z = 0$  and having surface charge  $\sigma e$  sees on its right ( $z > 0$ ) an integrated charge  $\sigma e - qe \int_0^d \rho(z) dz = -\sigma e$  from electro-neutrality, that is thus of opposite sign. The contact theorem (1) is exact, and remains true when the counterion excluded volume is accounted for. We note that it implies a strong constraint on the contact density  $\rho(0)$  of an isolated macromolecule. Indeed, when  $d \rightarrow \infty$ , the pressure  $P$  should vanish so that eq. (1) implies  $\rho(0) = 2\pi\ell_B\sigma^2$ . This result shows that the contact density does not depend on the valency  $q$  of ions. When  $d$  is finite, it is no longer possible to know  $\rho(0)$  without an explicit and often complicated statistical-mechanics treatment, and the ensuing pressure is a non-trivial quantity. It however only depends on 2 parameters (a reduced distance plus a coupling parameter) and we shall see that for strongly correlated systems, meaning for instance that  $\sigma$  is large, and for small enough  $d$ ,  $\rho(0)$  becomes simple again and yields an interesting equation of state through (1). Before addressing that small  $d$  situation, it is informative to discuss in more details the case where the two plates are at a large distance from each other.

### 3. – The large distance limit

When  $d$  is large (meaning  $d \gg a$ , where  $a$  is the lateral correlation length which we are about to define), the ionic distribution  $\rho(z)$  around a macromolecule is only weakly affected by the presence of the other plate. We have furthermore emphasised in the introduction that the relevant situation for like-charge attraction is that where non-mean-field effects are at work, so that the electrostatic coupling should be large enough. To quantify such a coupling, one can assume that all ions are collapsed onto the plate

(which happens at low enough temperature), in which case the mean surface per counterion is  $q/\sigma$ , which defines a typical distance  $a \propto \sqrt{q/\sigma}$  between ions. Comparing their typical Coulombic repulsion  $q^2 e^2 / (\epsilon a)$  to  $kT$ , we obtain the ratio

$$(2) \quad \frac{q^2 e^2}{\epsilon a} \frac{1}{kT} \propto \frac{e^2}{\epsilon kT} q^2 \frac{\sigma^{1/2}}{q^{1/2}} = (q^3 \ell_B^2 \sigma)^{1/2}.$$

Taking the square, we define the coupling constant  $\Xi = 2\pi q^3 \ell_B^2 \sigma$  [13, 14]. This parameter discriminates weakly coupled cases where  $\Xi \ll 1$  and mean field holds, from strongly coupled ones, where  $\Xi \gg 1$  [13, 15, 14]. Large couplings may be obtained in practice by increasing  $\sigma$  or  $q$  (considering multivalent ions such as  $\text{Cr}^{3+}$ , spermidine $^{3+}$  having  $q = 3$ , or spermine $^{4+}$  with  $q = 4$ .)

In the subsequent analysis, we consider  $\Xi \gg 1$ , where the counterions form a quasi-2D layer around the (still here isolated) plate: indeed, they are then in a configuration close to the ground state, which is a hexagonal two-dimensional crystal, the so-called Wigner crystal [16]. In the ground state ( $T = 0$  or equivalently  $\Xi = \infty$ ), it should be noted that any counterion feels the electric field created by the plate, while the field due to other counterions vanishes by symmetry: all ions lie in the same plane. Hence, due to thermal excitations and provided  $d$  is small enough, the ions can move slightly away from the plate and explore a region of size  $\mu$ , where the energy cost for exciting a given ion, to leading order in  $kT$ , stems entirely from the plate potential. Remembering that the bare plate creates for  $z > 0$  an electrostatic potential  $-2\pi \sigma e z / \epsilon$ , we can therefore estimate the value of  $\mu$  by writing

$$(3) \quad qe \frac{2\pi}{\epsilon} \sigma e \mu = kT \quad \implies \quad \mu = \frac{1}{2\pi q \ell_B \sigma}.$$

It is instructive to compare this new length scale  $\mu$ , called the Gouy length, to both  $a$  and  $\ell_B$  [17]: from the condition  $\Xi \gg 1$ , we infer that

$$(4) \quad \mu \ll a \ll q^2 \ell_B \quad \text{and more precisely} \quad \frac{\mu}{a} \propto \frac{a}{q^2 \ell_B} \propto \frac{1}{\sqrt{\Xi}}.$$

The corresponding configuration is shown in fig. 2. We now ascertain the consistency of neglecting the field due to other counterions on a given one: if the contribution due to other ions is accounted for, we obtain that an ion moved from its ground-state position experiences an additional potential in  $q^2 z^2 / (\epsilon a^3)$ . For  $z = \mu$ , this yields  $kT \ell_B \mu^2 / a^3 \propto kT \Xi^{-1/2} \ll kT$ . Here as in most of our discussion, the requirement of a large  $\Xi$  is paramount<sup>(1)</sup>.

---

<sup>(1)</sup> These arguments immediately provide the ion density profile around an isolated charged plate, showing that as far as the  $z$  coordinate is concerned and to leading order in  $\Xi$ , the ions decouple from each other, thereby forming an ideal gas in an external gravitational-like field. The ensuing profile is simply [18-21]  $\rho(z) \propto \exp(-z/\mu)$ . This expression should become

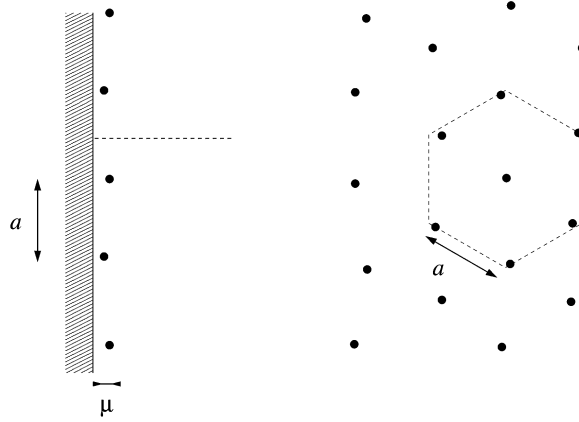


Fig. 2. – Left: Side view of the ionic atmosphere in the vicinity of a single charged plate (large  $d$  limit). The large value of the coupling parameter  $\Xi$  makes that  $\mu \ll a$ . Right: Front view of the system. When  $T = 0$  (*i.e.*  $\Xi = \infty$  and the Gouy length  $\mu = 0$ ), the counterions are exactly located on the hexagonal lattice with constant  $a$ . At finite but large  $\Xi$  (the situation shown), the counterions are close to these limiting positions.

Seen from a large distance by an infinitesimal test charge moving along the  $z$ -axis as shown by the dashed line in fig. 2, left, the whole structure (plate+ions) does not create any electric field since it is electro-neutral (more precisely, the electric field is exponentially small for  $z \gg a$ , and decays like  $\exp(-z/a)$ ). However, when the test charge is close to the plate ( $z \ll a$ ), and assuming it does not sit on a counterion but at maximum possible distance from counterions (see the dashed line in fig. 2, left), the electric field is that of the bare plate,  $2\pi\sigma z/\epsilon$ . This innocuous remark plays an important role in the argument to follow.

#### 4. – From infinite to small inter-plate distances: the unbinding scenario

In light of the previous discussion, it is only when  $d$  becomes smaller than the lateral correlation length  $a$  that the ionic structure on a plate starts to distort compared to the infinite separation case (this expectation is fully corroborated by a detailed analysis [22]). The problem then becomes complex, except when  $d \ll a$ , see fig. 3. In this short separation limit, the ions are confined to a quasi-2D geometry and we need to identify

---

asymptotically exact when  $\Xi \rightarrow \infty$  —as validated by numerical simulations— entailing that the profile should obey the contact theorem, valid at all couplings. This is indeed the case: from normalisation, it follows that  $\rho(z) = 2\pi\ell_B\sigma^2 \exp(-z/\mu)$  so that  $\rho(0) = 2\pi\ell_B\sigma^2$ . It should not be forgotten though that the ideal-gas picture only holds for the  $z$  degree of freedom, whereas the ions strongly repel in the perpendicular direction (parallel to the plate), where they form a crystal.

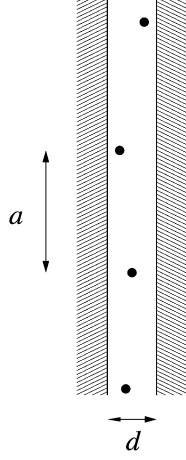


Fig. 3. – The two plates in the small separation limit. It is assumed here that  $d \ll a$ , which can still be compatible with  $\mu \ll d$ , see eq. (4).

the position of a given counterion by its projection parallel to the plates  $\mathbf{r}_{\parallel}$ , and its coordinate  $z$ . Both coordinates should be considered separately. Projecting the structure onto a plate, thereby eliminating  $z$  and focussing onto the set of  $\mathbf{r}_{\parallel}$  for all ions, we obtain a Wigner crystal very reminiscent of that sketched in fig. 2,right, with the only difference that the surface density of ions is now doubled, and that the lattice constant is hence changed according to  $a \rightarrow a/\sqrt{2}$ . On the other hand, the behaviour of the  $z$  coordinate is more subtle.

A given counterion in the slab experiences the sum of the potentials created by the plates plus a term due to counterions interactions. The first plates-ion contribution yields a vanishing electric field (constant potential, say 0) in the symmetric plate case. As for the second ion-ion interaction and as was the case for the single-plate analysis of sect. 3, it is a small quantity since all counterions basically lie in the same plane, with an ensuing small electric field created. To be more specific, this interionic energy per particle can be estimated as being of order  $kT\ell_B d^2/a^3 \propto kT (d/a)^2 \Xi^{1/2}$ ; it is thus small compared to  $kT$  provided that  $d/a \ll \Xi^{-1/4}$  or equivalently  $d/\mu \ll \Xi^{1/4}$ . Under that proviso, we can neglect the ion-ion interactions: the ions then experience a uniform potential, freely explore the available space  $0 \leq z \leq d$ , and consequently adopt a uniform density profile along  $z$ :  $\rho(z) = \text{constant}$ . From normalisation  $\int \rho dz = 2\sigma/q$  and we necessarily have  $\rho(z) = 2\sigma/(qd)$ . There is consequently an *unbinding* of ions which takes place: when  $d$  is large, the ions are confined in a narrow region of extension  $\mu$  around each plate, see sect. 3. When  $d \ll a$ , the counter-ions unbind from the plates, along the  $z$ -direction, as a consequence of the (nearly) cancellation of inter-ionic interactions, and can explore the full slab width, of extension  $d$ . Note that  $d$  can be larger than  $\mu$ , while being small compared to  $a/\Xi^{1/4}$ , see eq. (4). Still, in the transverse direction  $\mathbf{r}_{\parallel}$ , the ions are strongly correlated and are essentially frozen on the hexagonal Wigner positions.

Taking advantage of the unbinding phenomenon, the last ingredient of the analysis is to recall the contact theorem which allows to cast the interplate pressure in the form

$$(5) \quad \frac{P}{kT} = \frac{2\sigma}{qd} - \frac{2\pi\sigma^2 e^2}{\epsilon kT} = 2\pi\ell_B\sigma^2 \left( \frac{2\mu}{d} - 1 \right).$$

Thus, when  $d > 2\mu$ , the pressure is negative, and the two like-charge plates attract. On the other hand, when  $d < 2\mu$ , the pressure is repulsive and its positive sign stems from the penalising entropy for confining ions in too narrow a slab, which becomes overwhelming and leads to the divergence  $P \sim 2\sigma kT/(qd)$  when  $d \rightarrow 0$ . It can be pointed out that a systematic expansion in inverse powers of the (large) coupling parameter  $\Xi$  completely confirms our argument [21, 23], and provides the following correction to the equation of state (eq. (5))

$$(6) \quad \frac{P}{kT} = 2\pi\ell_B\sigma^2 \left( \frac{2\mu}{d} - 1 + \frac{d}{a} 0.6672 \dots + \mathcal{O}(d^2/a^2) \right).$$

Here, the same requirement as above holds for  $d/a$ , namely that  $d/a \ll \Xi^{-1/4}$ . The term  $d/a$  in the parenthesis in eq. (6) is therefore a small correction compared to the others. Expression (6) shows that the ion-ion interactions that were neglected in deriving eq. (5) contribute to a small correction, as expected. In other words, the true density profile, leading to (6) via the contact theorem, is not exactly flat as considered, but slightly peaked in the vicinity of the plates<sup>(2)</sup> [21, 23]. In this respect, the equation of state (5) is necessarily a lower bound for the pressure. It is all the more accurate as the condition  $d \ll a/\Xi^{1/4}$  is met, and since we may have  $\mu \ll d$ ,  $P$  may take values close to the maximally attractive bound  $-2\pi\sigma^2 e^2/\epsilon$ . This is a key point explaining the stability of cement pastes [24], that can be viewed to first approximation as made up of parallel charged plates with intercalated multivalent ions.

## 5. – Discussion

We now examine in more details some questions raised by our treatment, together with a possible generalisation.

**5.1. Unbinding scenario and ground-state structure.** – The argument put forward in sect. 4 for like-charge attraction hinges upon the unbinding of ions from the near vicinity of the plates, which leads to a uniform  $\rho(z)$  profile across the slab. We have argued that this could occur at large  $\Xi$  provided  $d \ll a/\Xi^{1/4}$ , but it is clear that such a flat profile is far from the ground-state structure of the bilayer. Indeed, Earnshaw theorem states that an equilibrium position cannot be obtained in a system of point charges under the action of electrostatic forces alone [25]. This means here that the counterions stick to

---

<sup>(2)</sup> These two small peaks are precursors of their ground-state counterpart, that develop when  $\Xi \gg (a/d)^4$ , see the discussion in sect. 5.1.

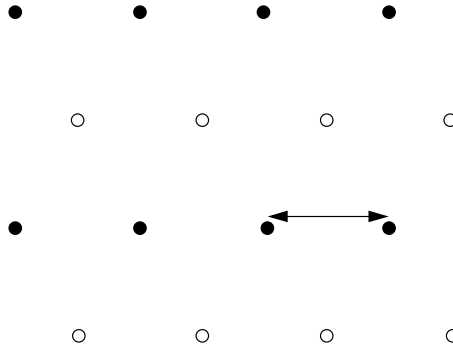


Fig. 4. – Front view of the ground-state structure for  $d \ll a$ . The structure is a hexagonal crystal of lattice constant  $a/\sqrt{2}$  (shown by the double arrow), where the open and filled symbols correspond to counterions in contact with the plate at  $z = 0$  or at  $z = d$ , respectively.

the plates when  $T = 0$ , and a more refined study reveals that charges adopt the pattern shown in fig. 4 [26, 22]. The corresponding  $\rho(z)$  profile is thus a sum of two  $\delta$  peaks at  $z = 0$  and  $z = d$ , very non-uniform. . . There is of course no incompatibility between our uniform smooth profile and the correct singular ground state. When the interplate distance  $d$  and  $a$  are fixed (note that both length scales are temperature independent, unlike the Gouy length), and  $T$  is decreased to 0 in order to realize the ground state,  $\Xi$  increases and the condition  $d \ll a/\Xi^{1/4}$  is violated at some point. There is then a crossover between the flat profile and the strongly peaked one that is reached in the ground state. In other words, the analysis of sect. 4 is valid for large  $\Xi$ , but nevertheless requires that  $\Xi \ll (a/d)^4$ . By working with suitably rescaled quantities, it is nevertheless possible to obtain expression that are strictly speaking correct for  $\Xi \rightarrow \infty$ , see below.

**5.2. Back to the failure of mean-field.** – It is informative to go back to the mean-field treatment, the Poisson-Boltzmann (PB) theory [13], which always predicts repulsion between the plates [6-8]. Yet, the contact theorem that has been used here, is obeyed by Poisson-Boltzmann profiles. Furthermore, the mean-field profile also becomes flat for small enough  $d$ . So, what is going on? The answer simply lies in the fact the length scale  $a$  has no counterpart in the mean-field approach, where the counterions are accounted for via their profiles, while discarding their discrete nature. As a consequence, it is only for  $d \ll \mu$  that the PB profile becomes flat [27]. Hence, the equation of state (5) also holds for PB theory, but only when  $d \ll \mu$ , a regime where  $P > 0$ .

This leads us to a second remark. It is often stated that PB theory becomes correct when  $\Xi$  is small enough (see, *e.g.*, [29] for a proof in a system having both co- and counter-ions). Loosely speaking, this is true, but some phenomena are governed in the real system (say in a simulation) by the length scale  $a$ , and are therefore necessarily missed at PB level, no matter how small  $\Xi$  is. This is illustrated in fig. 5, which shows pressures obtained in Monte Carlo simulations for three different coupling parameters,  $\Xi = 0.5$ ,  $\Xi = 100$  and  $\Xi = 10^5$ . The curve for  $\Xi = 0.5$  is close to the PB result shown by

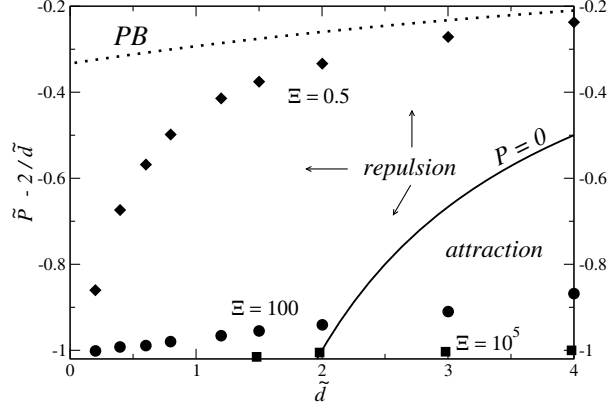


Fig. 5. – Rescaled and shifted equation of state as a function of rescaled distance:  $\tilde{P} - 2/\tilde{d}$  is plotted versus  $\tilde{d}$ , with  $\tilde{P} = P/(kT2\pi\ell_B\sigma^2)$  and  $\tilde{d} = d/\mu$ . The symbols show the Monte Carlo data of ref. [28]: the diamonds are for  $\Xi = 0.5$  (relatively weak coupling), the circles are for  $\Xi = 100$  (moderately strong coupling) and the squares are for  $\Xi = 10^5$  (very strong coupling). The Poisson-Boltzmann (mean-field) result is shown by the upper dotted line. The continuous curve displays the locus of points where  $P = 0$ . Hence, below this curve, the like-charge plates attract.

the dotted line provided  $d$  is not too small, see also fig. 6. For  $\Xi = 0.5$ , we have  $a \simeq \mu$ , and we see that the Monte Carlo data depart from the PB prediction for  $\tilde{d} < 1$ , *i.e.*

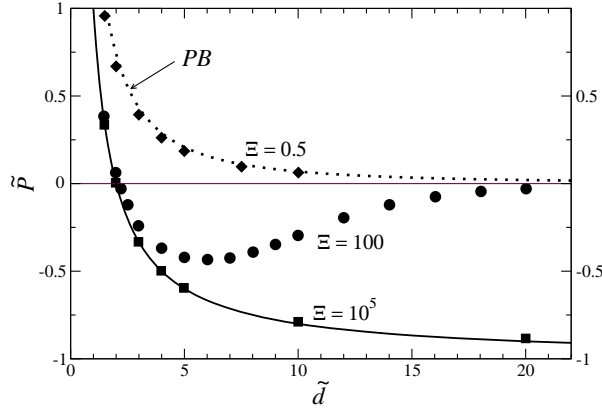


Fig. 6. – Rescaled equation of state  $\tilde{P}$  versus  $\tilde{d}$ . The symbols are for the Monte Carlo data of ref. [28] and have the same meaning as in fig. 5. They correspond to the numerical evaluation of  $P_{\text{exact}}$ . The Poisson-Boltzmann pressure is again shown by the dotted curve and the thick line displays the equation of state (eq. (7)).

$d < a$ . In the rescaled units used in the figure, our equation of state (5) reads

$$(7) \quad \tilde{P} = \frac{2}{\tilde{d}} - 1.$$

Interestingly, for  $d \ll a$  and  $\Xi = 0.5$  (upper symbols) we see that our expression is perfectly obeyed, since  $\tilde{P} - 2/\tilde{d} \rightarrow -1$ . Indeed, the requirement of a flat profile is met for  $d \ll \mu$ . On the other hand, the PB result is  $\tilde{P} - 2/\tilde{d} \rightarrow -1/3$  [19], as can be seen in the figure, which significantly departs from the simulation data. It can be concluded that eq. (5) or eq. (7) are not limited to strongly coupled systems, but also provide the limiting small  $d$  behaviour at arbitrary coupling  $\Xi$ . Yet, we emphasise that eq. (5) or eq. (7) only lead to attractive behaviour when  $\Xi$  is large (attraction requires having  $\mu \ll a$ ); for  $\Xi = 100$  or  $\Xi = 10^5$  and  $d > 2\mu$  ( $\tilde{d} > 2$ ) the pressure does indeed exhibit a negative sign: the circles and squares lie below the separatrix  $P = 0$  shown by the continuous curve in the lower right corner of fig. 5, see also fig. 6. Moreover, while eq. (5) is fairly well obeyed by the Monte Carlo data at  $\Xi = 100$ , the improved version eq. (6) fares better and is in good agreement with the simulation results, as discussed in detail in [23]. When the electrostatic coupling is increased even further, the agreement between simulations and eq. (5) becomes excellent, see figs. 5 and 6.

To finish with the scaling form (eq. (7)), we point out that from dimensional analysis, the exact rescaled inter-plate pressure can in general be written as a function of two arguments only, *i.e.*  $\tilde{P}_{\text{exact}}(\tilde{d}, \Xi)$ . This is true for all values of  $\Xi$ . Working at fixed  $\tilde{d}$  and letting  $\Xi \rightarrow \infty$  to enforce the strong-coupling limit, we obtain  $d/a \propto \tilde{d}\Xi^{-1/2}$  which is thus negligible compared to  $\Xi^{-1/4}$ . This means that

$$(8) \quad \lim_{\Xi \rightarrow \infty} \tilde{P}_{\text{exact}}(\tilde{d}, \Xi) = \frac{2}{\tilde{d}} - 1.$$

This is clearly illustrated in fig. 6. Of course, for larger distances than those in the figure, the pressure for  $\Xi = 10^5$  would start to deviate from the prediction (eq. (7)), since the criterion  $d/a \ll \Xi^{1/4}$  would no longer be met (in the present case,  $d/a \simeq \Xi^{1/4}$  corresponds to  $\tilde{d} \simeq 20$  indicating that deviations would start to appear for already  $\tilde{d}$  on the order of 50 or less). Incidentally, fig. 6 also highlights a) that PB holds for large enough distances under weak-coupling (diamonds,  $\Xi = 0.5$ ) and b) that for large enough  $\Xi$ , the pressure is negative provided  $\tilde{d} > 2$ . How large should  $\Xi$  be is not provided by our argument. It has been reported that  $\Xi_c \simeq 12$  is the threshold value below which no attraction is possible [28].

**5.3. Large distance behaviour.** – At this point, it is interesting to discuss the phenomenology for large distances. What is the sign of the pressure? We have repeatedly emphasised that our argument is limited to small enough distances, so that it is not informative for the large  $d$  physics. Worse than that, it appears that there is to date no reliable answer —be it experimental, numerical or analytical— to the question raised, and we are confined here to speculation. A plausible scenario is that when the two plates are

at a large distance from each other, the ionic profile far enough from the plates is dilute, so that the local coupling parameter is small in the interstitial region. Mean-field can be expected to hold there [18, 30, 31], from which we might infer that the large distance pressure should be positive. Hence, for a given coupling parameter  $\Xi$ , we may surmise a re-entrant behaviour, with a repulsive pressure at both small and large distances, and an attractive window in between. This expectation may be dimension-dependant, since a recent two-dimensional study of the same problem has shed doubts on the re-entrance of repulsion at large  $d$  [32]. It should be outlined though that the log-form Coulomb potential takes in two dimension is scale free, so that the coupling parameter in 2D is density independent ( $\beta q^2$  where  $\beta$  is the inverse temperature, which unlike  $\Xi$  does not depend on the macromolecule charge). This is a notable difference with 3D systems.

**5.4. Asymmetric plates generalisation.** – It is straightforward to extend our analysis to the situations where the two plates bear unequal surface charges. We leave the derivation as an exercise, emphasising that the main difference with the treatment put forward in sect. 4 is that the electric field created by the two plates is now non-vanishing, but still uniform. It is given by  $2\pi(\sigma_1 - \sigma_2)e/\epsilon$  where  $\sigma_i$  denotes the surface charge on plate  $i$  (plate 1 at  $z = 0$  and plate 2 at  $z = d$ ), from which we define the asymmetry parameter  $\zeta = \sigma_2/\sigma_1$ . We can again, for small interplate distance neglect the ion-ion interaction. The ions thus experience a linear potential, which leads to an exponential profile in  $\exp[-z(1 - \zeta)/\mu]$ , where  $\mu = \mu_1$  is the Gouy length of plate 1. Upon proper normalising the counterion profile ( $q \int \rho dz = \sigma_1 + \sigma_2$ ), and invoking once more the contact theorem which reads

$$(9) \quad P = \rho(0) kT - \frac{2\pi}{\epsilon} \sigma_1^2 e^2 = \rho(d) kT - \frac{2\pi}{\epsilon} \sigma_2^2 e^2,$$

we obtain [33, 23, 34]

$$(10) \quad \tilde{P} = \frac{P}{kT 2\pi \ell_B \sigma_1^2} = -\frac{1}{2}(1 + \zeta^2) + \frac{1}{2}(1 - \zeta^2) \coth\left(\frac{(1 - \zeta)d}{2\mu}\right).$$

This expression reduces to (5) when  $\zeta \rightarrow 1$ , as it should. An interesting check for the consistency of the approach is to verify that the same pressure is recovered no matter which plate is used for evaluating the pressure in eq. (9). Another interesting and exact consequence of the contact theorem (9) is that the interactions between a plate at arbitrary charge and a neutral one are always repulsive:  $\sigma_2 = 0$  leads to  $P = \rho(d) kT > 0$ .

## 6. – Conclusion

We considered two interacting parallel charged plates, forming a slab where neutralising counterions are confined. We have presented an argument to unveil the mechanisms behind the like-charge attraction that may ensue at large Coulombic coupling parameter  $\Xi$ , following a mechanical route whereas other approaches often rely on an energy route [35, 18, 13]. Our argument hinges upon the fact that at small enough interplate

separation, the counterions unbind from the vicinity of the plates. From the contact theorem, attraction can only set in when the counterion density at contact  $\rho(0)$  is below its large distance value, and the unbinding phenomenon is thereby the key to like-charge attraction. More precisely, a single counter-ion picture prevails, where due to strong lateral repulsion (parallel to the plates), the ions move in the perpendicular  $z$ -direction under the potential created by the plates only, as if they did not interact. This viewpoint is fruitful and efficient for the planar geometry considered, but it is misleading in two respects: first, it may lead to believe that while the single particle image provides the exact leading order pressure when  $\Xi \rightarrow \infty$ , the next correction in the  $\Xi$  expansion stems from two-body interactions, in a virial-like scheme. This is the essence of the virial approach of refs. [19, 28, 17], which has been shown to be incorrect [21, 23]. Second, the single particle picture is in general inappropriate, even to obtain the dominant behaviour at large  $\Xi$ . This appears most clearly when considering the ionic profile for a single plate defining two half spaces with different dielectric constants (work in preparation).

To dominant order in the coupling parameter  $\Xi$ , the fact that there is an underlying Wigner crystal of ions has no apparent signature on the interactions (this signature should be sought in the next to dominant term [21, 23]). However, the presence of the crystal is important for allowing the unbinding of ions and in this respect, the description of strongly coupled charged matter is in the realm of low temperature physics, as discussed in the review [20]. It is then instructive to remind the value of the coupling parameter where crystallisation occurs, which is on the order of  $\Xi_c \simeq 3 \cdot 10^5$  [36]. If strong coupling approaches of the Wigner kind, such as that leading to (6) where restricted to this range of coupling, they would be of little interest, since it is in practice difficult to exceed  $\Xi = 100$  (*e.g.*, trivalent counterions are required in water for already large surface charges such that  $\sigma \ell_B^2$  is of order 1 [17]). However, it has been shown that the predictions derived from the Wigner picture apply “down to” much smaller value than  $\Xi_c$ , such as 50 or sometimes less [23]. This means that the key point is not the crystal in itself, but the existence of a strong correlation hole around each counterion.

\* \* \*

The authors would like to acknowledge interesting conversations with Y. LEVIN, M. KANDUČ, J. P. MALLARINO, A. NAJI, R. NETZ R. PODGORNIK and G. TÉLLEZ.

## REFERENCES

- [1] BELLONI L., *J. Phys.: Condens. Matter*, **12** (2000) R549.
- [2] LEVINE S. and DUBE G., *Trans. Faraday Soc.*, **35** (1939) 1125.
- [3] VERWEY E. and OVERBEEK J., *Theory of The Stability of Lyophobic Colloids* (Elsevier Publishing Company, New York) 1948.
- [4] LEVINE S. and HALL D., *Langmuir*, **8** (1992) 1090.
- [5] OVERBEEK J., *Mol. Phys.*, **80** (1993) 685.
- [6] NEU J., *Phys. Rev. Lett.*, **82** (1999) 1072.
- [7] SADER J. and CHAN D., *Langmuir*, **16** (2000) 234.
- [8] TRIZAC E., *Phys. Rev. E*, **62** (2000) R1465.

- [9] GULDBRAND L., JÖNSON B., WENNERSTRÖM H. and LINSE P., *J. Chem. Phys.*, **80** (1984) 2221.
- [10] KJELLANDER R. and MARČELJA S., *Chem. Phys. Lett.*, **112** (1984) 49.
- [11] KÉKICHEFF P., MARČELJA S., SENDEN T. and SHUBIN V. E., *J. Chem. Phys.*, **99** (1993) 6098.
- [12] HENDERSON D., BLUM L. and LEBOWITZ J., *J. Electroanal. Chem.*, **102** (1979) 315.
- [13] LEVIN Y., *Rep. Prog. Phys.*, **65** (2002) 1577.
- [14] NAJI A., KANDUČ M., NETZ R. and PODGORNİK R., *Exotic electrostatics: Unusual features of electrostatic interactions between macroions*, in *Understanding Soft Condensed Matter via Modeling and Computation*, edited by ANDELMAN D. and REITER G. (Addison Wesley) 2010.
- [15] MESSINA R., *J. Phys.: Condens. Matter*, **21** (2009) 113102.
- [16] WIGNER E., *Phys. Rev.*, **46** (1934) 1002.
- [17] NAJI A., JUNGBLUT S., MOREIRA A. and NETZ R., *Physica A*, **352** (2005) 131.
- [18] SHKLOVSKII B., *Phys. Rev. E*, **60** (1999) 5802.
- [19] NETZ R., *Eur. Phys. J. E*, **5** (2001) 557.
- [20] GROSBURG A. Y., NGUYEN T. T. and SHKLOVSKII B. I., *Rev. Mod. Phys.*, **74** (2002) 329.
- [21] ŠAMAJ L. and TRIZAC E., *Phys. Rev. Lett.*, **106** (2011) 078301.
- [22] ŠAMAJ L. and TRIZAC E., *Phys. Rev. B*, **85** (2012) 205131.
- [23] ŠAMAJ L. and TRIZAC E., *Phys. Rev. E*, **84** (2011) 041401.
- [24] PELLENCQ R.-M., CAILOL J.-M. and DELVILLE A., *J. Phys. Chem. B*, **101** (1997) 8584.
- [25] EARNSHAW S., *Trans. Cambridge Philos. Soc.*, **7** (1842) 97.
- [26] GOLDONI G. and PEETERS F. M., *Phys. Rev. B*, **53** (1996) 4591.
- [27] ANDELMAN D., *Introduction to electrostatics in soft and biological matter*, in *Soft Condensed Matter Physics in Molecular and Cell Biology*, edited by POON W. and ANDELMAN D. (Addison Wesley) 2006, Ch. 6.
- [28] MOREIRA A. and NETZ R., *Eur. Phys. J. E*, **8** (2002) 33.
- [29] KENNEDY T., *J. Stat. Phys.*, (1984) 529.
- [30] CHEN Y.-G. and WEEKS J., *Proc. Natl. Acad. Sci. U.S.A.*, **103** (2006) 7560.
- [31] DOS SANTOS A., DIEHL A. and LEVIN Y., *J. Chem. Phys.*, **130** (2009) 124110.
- [32] ŠAMAJ L. and TRIZAC E., *Eur. Phys. J. E*, **34** (2011) 20.
- [33] KANDUČ M., TRULSSON M., NAJI A., BURAK Y., FORSMAN J. and PODGORNİK R., *Phys. Rev. E*, **78** (2008) 061105.
- [34] PAILLUSSON F. and TRIZAC E., *Phys. Rev. E*, **84** (2011) 011407.
- [35] ROUZINA I. and BLOOMFIELD V., *J. Phys. Chem.*, **100** (1996) 9977.
- [36] BAUS M. and HANSEN J.-P., *Phys. Rep.*, **59** (1980) 1.